ORIGINAL ARTICLE

Electromagnetic Torque Characteristics Analysis of Nuclear Half-Speed Turbine Generator with Stator Winding Inter-Turn Short Circuit Fault

Peng Xin[1] · Baojun Ge[2] · Dajun Tao[2] · Pin Lv[3]

Abstract

To research the variation characteristics and influence factors of air gap magnetic field and electromagnetic torque of nuclear power half-speed turbine generator with stator winding inter-turn short circuit, the two-dimensional transient electromagnetic field of generator-external circuit-grid coupling mathematical model is established by field-circuit-network coupling method. Taking the national laboratory's generator as an example, and comparing the simulation results of the inter-turn short circuit of the armature winding with experimental data, the correctness of the model is validated. On this basis, the simulation model of a 1407MVA nuclear power half-speed turbine generator is built. Then the stator winding inter-turn short circuit fault is simulated when the generator is connected to the grid with rated load. The characteristics of air gap flux density and electromagnetic torque are obtained before and after fault, as well as, the relationship between their each component and the fault degree is obtained. At the same time, the variation law of air gap flux density and electromagnetic torque is obtained when the relative position between fault winding and magnetic pole changes. The theoretical reference for fault diagnosis and localization using harmonic electromagnetic torque after fault is provided.

Keywords Nuclear power half-speed turbine generator · Field-circuit-network coupling · Inter-turn short circuit · Air gap flux density · Electromagnetic torque

1 Introduction

As an important part of the power system, the safe and stable operation of large generators has always been a hot issue for many researchers. As one of the common faults of generator, the stator winding inter-turn short circuit fault of large generator can cause electromagnetic noise and radial vibration when the fault occurs. When the fault is serious, it can cause stator core damage and a series of problems [1]. Therefore, it is of practical significance to research the inter-turn short

✉ Peng Xin
  xinpeng4321@163.com

1 College of Information and Control Engineering, Jilin Institute of Chemical Technology, Jilin 132022, Jilin, China

2 College of Electrical and Electronic Engineering, Harbin University of Science and Technology, Harbin, Heilongjiang, China

3 College of Electrical and Control Engineering, Heilongjiang University of Science and Technology, Harbin, Heilongjiang, China

circuit of generator stator winding to ensure the safe and stable operation of the generator.

Scholars have done some research work on the inter turn short circuit fault of generator stator winding. In reference [2], the influence of stator winding inter-turn short circuit position on the electromagnetic torque fluctuation characteristics is studied when the air gap of synchronous generator is eccentric. It is pointed out that the angle between the electromagnetic torque and the position of short circuit and minimum air gap is approximately cosine. In reference [3], the influence of stator winding inter-turn short circuit on the induction electromotive force of generator is studied, and the potential difference before and after the fault is proposed to diagnose the fault. In reference [4–7], the vibration characteristics and the influencing factors of the generator after inter-turn short circuit under different working conditions are studied. In reference [8], a new detecting coil method for detecting the inter-turn short circuit fault of generator winding is proposed. In reference [9], the variation characteristics of negative sequence current component after stator winding inter-turn short circuit fault are studied. In reference [10], the field circuit coupling method is used to

study the dynamic electromagnetic force distribution on the top and the wall of the rotor teeth when the stator winding turns are short circuited. In reference [11], single winding analysis and finite element analysis are used to study the characteristics of inter-turn short circuit fault of generator stator winding. It is pointed out that short circuit current, phase current, torque and radial force are related to fault location and fault degree. In reference [12, 13], the variation characteristics of air gap magnetic field and electromagnetic torque in case of rotor vibration eccentricity and stator winding inter-turn short circuit fault are studied. It shows that the second harmonic vibration changes obviously after the fault. It is proposed to detect the eccentricity of the rotor by using the 17th and 19th harmonic currents. In reference [14], the field circuit coupling method is used to study the distribution of eddy current loss on the rotor surface after inter-turn short circuit of generator stator winding.

The above references have made some achievements in the research of generator stator winding inter-turn short circuit fault. However, in most of the above references, the research on electromagnetic torque is only limited to fault identification. The change rule and influence factors of each harmonic component of electromagnetic torque after fault are not analyzed in depth. Therefore, it is necessary to study the characteristics of electromagnetic torque in the case of inter-turn short circuit fault in the stator winding of nuclear generator. Based on the above references, taking a large nuclear power half speed turbo-generator as the research object, and adopting the field circuit network coupling method, it is established that a coupled simulation model for the operation of nuclear power generator with rated load in grid. On this basis, the inter-turn short circuit fault of the stator winding is simulated. The variation characteristics of internal magnetic field and electromagnetic torque before and after fault are studied. The variation law of the components of air gap flux density and electromagnetic torque after fault is given. It is pointed out that there is a one-to-one relationship between the relative position of the fault winding to the pole and harmonic components of the electromagnetic torque. The research results provide theoretical reference for the diagnosis and location of stator winding inter-turn short circuit fault.

2 Field-Circuit-Network Coupled Mathematical Model

Taking the one machine infinite bus system as the research object, the equivalent circuit of the system is shown in Fig. 1.

2.1 Generator Magnetic Field Equation

It is assumed that the permeability and conductivity of iron core are considered as isotropic, the magnetic field of generator is quasi-static field, the displacement current and the eddy current loss of stator core are ignored. The boundary-value problem of the generator 2D transient electromagnetic field is written as

$$\begin{cases} \Omega : \frac{\partial}{\partial x}\left(\frac{1}{\mu}\frac{\partial A}{\partial x}\right) + \frac{\partial}{\partial y}\left(\frac{1}{\mu}\frac{\partial A}{\partial y}\right) = -J + \sigma\frac{dA}{dt} \\ \Gamma : A = 0 \end{cases} \tag{1}$$

where μ is magnetic permeability, J is source current density, σ is electrical conductivity, and A is magnetic vector potential, Γ is the boundary of the outer circle of stator and the inner circle of rotor.

2.2 Mathematical Model of Generator

2.2.1 Generator Stator Winding Loop Equation

As shown in Fig. 1, the generator stator winding loop equation can be expressed as

$$\begin{aligned} U_s &= E_s - R_s I_s - L_s \frac{dI_s}{dt} \\ &= -l_{ef} C_s^T \frac{\partial A}{\partial t} - R_s I_s - L_s \frac{dI_s}{dt} \end{aligned} \tag{2}$$

where E_s is the induction electromotive force of generator, $E_s = [e_a, e_b, e_c]^T$, U_s and I_s are the armature terminal voltage and current respectively, $U_s = [u_A, u_B, u_C]^T$, $I_s = [i_A, i_B, i_C]^T$, R_s and L_s are stator winding resistance matrix and end leakage inductance matrix respectively, $R_s = diag[R_s, R_s, R_s]^T$, and $L_s = diag[L_s, L_s, L_s]^T$, l_{ef} is the effective axial length
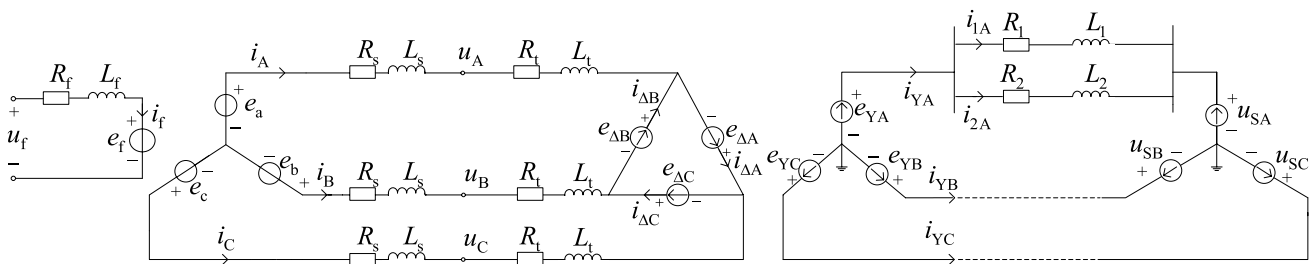

Fig. 1 Equivalent circuit of one machine infinite bus system

of the generator, and C_s is the incidence matrix of stator current.

The current density of stator winding is as follows:

$$J_s = \frac{i_s}{a} \cdot \frac{1}{S_s} \qquad (3)$$

where i_s is the phase current of stator winding, a is the number of parallel branches of stator winding, and S_S is the sectional area of stator winding.

2.2.2 Excitation Loop Equation

As shown in Fig. 1, the excitation loop equation can be expressed as

$$
\begin{aligned}
u_f &= e_f + R_f i_f + L_f \frac{di_f}{dt} \\
&= -l_{ef} C_f^T \frac{\partial A}{\partial t} + R_f i_f + L_f \frac{di_f}{dt}
\end{aligned}
\qquad (4)
$$

where u_f is excitation voltage, e_f is induced electromotive force of excitation winding, i_f is excitation current, R_f and L_f are excitation winding resistance and end leakage inductance respectively, and C_f is the correlation matrix of excitation current.

The current density of excitation winding is as follows:

$$J_f = i_f / s_f \qquad (5)$$

where S_f is the sectional area of excitation winding.

2.2.3 Damping Loop Equation

The schematic diagram of damping circuit is shown in Fig. 2. In the figure, R_{di} and L_{di} are the resistance and leakage inductance of the damping end ring respectively, R_{zi} and L_{zi} are the resistance and inductance of the damping winding, R_{wi} and L_{wi} are the slot wedge resistance and inductance, i_{bi} is the sum of the damping bar and slot wedge current; i_{di} is the loop current; u_{di} is the voltage at both ends of the damping bar.

Suppose that J_{ci} and J_{zi} are the current density of the straight line part of the wedge and the damping bar respectively, then

$$
\begin{cases}
J_{ci} = -\sigma_1 \frac{\partial A}{\partial t} + \sigma_1 \frac{u_{di}}{l_{ef}} \\
J_{zi} = -\sigma_2 \frac{\partial A}{\partial t} + \sigma_2 \frac{u_{di}}{l_{ef}}
\end{cases}
\qquad (6)
$$

where σ_1 and σ_2 are the electrical conductivity of the slot wedge and damping bar respectively.

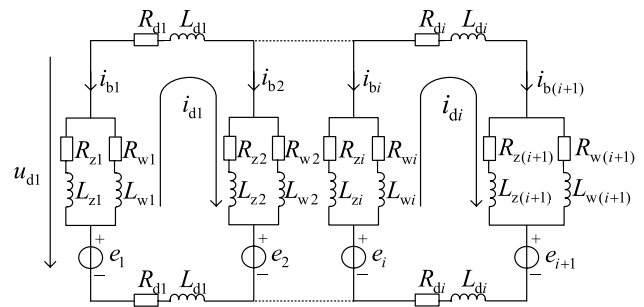The damping loop equation can be expressed as [15]

Fig. 2 Schematic diagram of damping circuit

$$
\begin{cases}
C_{d1} U_d + C_{d2} I_d + D_{d1} \frac{\partial A}{\partial t} = 0 \\
C_{d3} U_d + C_{d4} I_d + D_{d2} \frac{dI_d}{dt} = 0
\end{cases}
\qquad (7)
$$

2.2.4 Rotor Core Eddy Current

For the hydro generator, the rotor is composed of laminated form, so the eddy current effects can be neglected. For turbo generator, its rotor is solid, therefore, it can be treated by the method of modifying conductivity of iron core linear part [16].

$$J_R = -\sigma_R \frac{\partial A}{\partial t} \qquad (8)$$

where σ_R is the rotor material conductivity.

2.3 Mathematical Model of Power Grid

2.3.1 Transformer Equation

The transformer which is connected to the generator adopts Dyn11 connection form. As shown in Fig. 1, the voltage and the current equations of transformer can be written as

$$E_t = k G_1 \left(U_s - R_t I_s - L_t \frac{dI_s}{dt} \right) \qquad (9)$$

$$I_t = k G_2 I_t \qquad (10)$$

where E_t is voltage on HV side of transformer, I_t is current on HV side of transformer, k is the transformation ratio, $E_t = [e_{YA}, e_{YB}, e_{YC}]^T$, $I_t = [i_{YA}, i_{YB}, i_{YC}]^T$, R_t and L_t are transformer winding resistance matrix and end leakage inductance matrix respectively, $R_t = diag[R_t, R_t, R_t]$,

$L_t = diag[L_t, L_t, L_t]$, $G_1 = \begin{bmatrix} 1 & 0 & -1 \\ -1 & 1 & 0 \\ 0 & -1 & 1 \end{bmatrix}$, and

$G_2 = \begin{bmatrix} 1 & -1 & 0 \\ 0 & 1 & -1 \\ -1 & 0 & 1 \end{bmatrix}$.

2.3.2 Transmission Line Voltage and Current Equations

As shown in Fig. 1, the transmission line voltage and current equations can be written as

$$\begin{cases} E_t = U + R_1 I_1 + L_1 \dfrac{\mathrm{d}I_1}{\mathrm{d}t} \\ \quad = U + R_2 I_2 + L_2 \dfrac{\mathrm{d}I_2}{\mathrm{d}t} \end{cases} \tag{11}$$

$$I_L = I_1 + I_2 \tag{12}$$

where U and I_L are the infinite system voltage and current respectively, $U = [u_{SA}, u_{SB}, u_{SC}]^T$, $I_L = [i_{1A} + i_{2A}, i_{1B} + i_{2B}, i_{1C} + i_{2C}]^T$, R_1, R_2, L_1 and L_2 are their diagonal matrices respectively. If the transmission line is a single circuit transmission line in the system, then $I_2 = 0$.

Bringing Eqs. (3), (5), (6) and (8) into Eq. (1), after finite element discrimination, then

$$KA + C_s I_s + C_f I_f + C_{d5} U_d + D_{d3} \frac{\partial A}{\partial t} = 0 \tag{13}$$

Coupling Eqs. (2), (4), (7), (9)–(13), and eliminating the intermediate variables, the finite element equation can be got.

$$\begin{bmatrix} K & C_s & C_f & C_{d5} & 0 & 0 & 0 \\ 0 & 0 & R_f & 0 & 0 & 0 & 0 \\ 0 & 0 & 0 & C_{d1} & C_{d2} & 0 & 0 \\ 0 & 0 & 0 & C_{d3} & C_{d4} & 0 & 0 \\ 0 & -kG_1(R_s + R_t) & 0 & 0 & 0 & -R_1 & 0 \\ 0 & -kG_1(R_s + R_t) & 0 & 0 & 0 & 0 & -R_2 \\ 0 & -M & 0 & 0 & 0 & kG_2 & kG_2 \end{bmatrix} \begin{bmatrix} A \\ I_s \\ I_f \\ U_d \\ I_d \\ I_1 \\ I_2 \end{bmatrix} + $$

$$\begin{bmatrix} D_{d3} & 0 & 0 & 0 & 0 & 0 & 0 \\ -l_{ef}C_f^T & 0 & L_f & 0 & 0 & 0 & 0 \\ D_{d1} & 0 & 0 & 0 & 0 & 0 & 0 \\ 0 & 0 & 0 & 0 & D_{d2} & 0 & 0 \\ -kl_{ef}G_1 C_s^T & -kG_1(L_s + L_t) & 0 & 0 & 0 & -L_1 & 0 \\ -kl_{ef}G_1 C_s^T & -kG_1(L_s + L_t) & 0 & 0 & 0 & 0 & -L_2 \\ 0 & 0 & 0 & 0 & 0 & 0 & 0 \end{bmatrix} \frac{\partial}{\partial t} \begin{bmatrix} A \\ I_s \\ I_f \\ U_d \\ I_d \\ I_1 \\ I_2 \end{bmatrix} = \begin{bmatrix} 0 \\ u_f \\ 0 \\ 0 \\ U \\ U \\ 0 \end{bmatrix} \tag{14}$$

where $M = \text{diag}[1, 1, 1]$.

3 Simulation and Experiment

In this section, taking the MJF-30-6 non-salient pole synchronous generator in the national laboratory as an example, the simulation model is built. In the simulation model, the synchronous generator is connected with the infinite system through the transformer and the double circuit transmission line. When the generator is stable operation with 1/2 rated load, it is simulated that phase A winding first branch of generator occurs 2% to 22% inter-turn short circuit fault in 3 s. The fault is removed after 0.1 s, then, the generator returns to normal operation.

At the same time, in order to verify the correctness of the simulation model, the related experiment is carried out. In the experiment, the MJF-30-6 non-salient pole synchronous generator is connected with 11 kV grid through the transformer. The voltage step-up ratio of transformer is 2.5. And the connection group of transformer is Dyn11. In the experiment, the LM-1 excitation device and F6-10,000 special recording wave analysis device for experiment are used. The experiment site is shown in Fig. 3. And the simulation and experiment results are shown in Fig. 4.

As seen from Fig. 4, the simulation result of stator winding current is in agreement with the experiment result. The correctness of the simulation model is verified.

4 Harmonic Analysis of Air Gap Magnetic Field in Stator Winding with Inter-turn Short Circuit

In order to study the characteristics of inter-turn short circuit in stator winding of nuclear generator, the field-circuit-network coupled simulation model is established based on the case of a 1407MVA nuclear half speed turbo-generator connected to the infinite system with rated load. In this model, the generator is connected with the infinite system through the transformer and the double circuit transmission line. The generator is modeled by finite element method, and the influence of structure and magnetic saturation are fully considered in the modeling process. Main parameters of generator are shown in Table 1:

Fig. 3 Experiment site
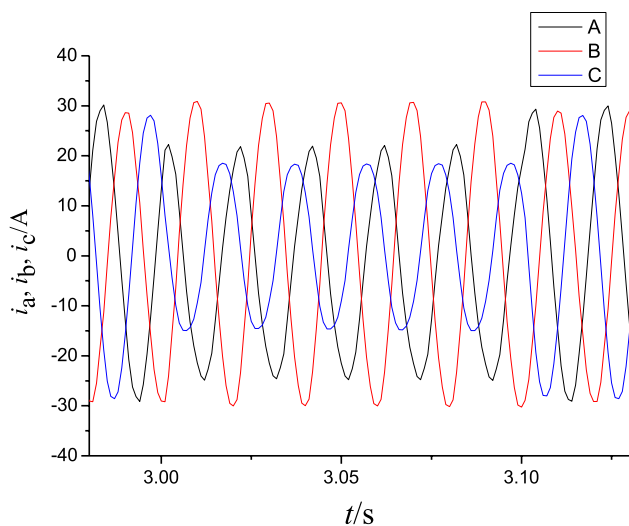
(a) Simulation results of stator current
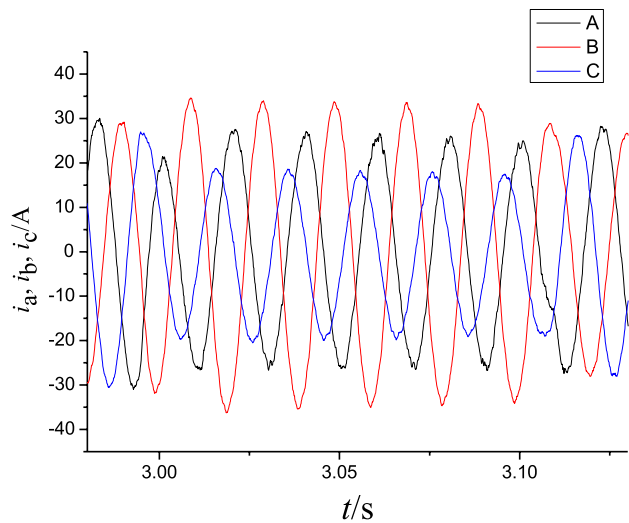
(b) Experiment results of stator current

Fig. 4 Comparison between stator current simulation result and experimental result

In order to improve the accuracy of the calculation, the layered mesh generation method is adopted in the air gap mesh generation. The meshing result is shown in Fig. 5.

Under the condition of stable operation of nuclear power generator with rated load, 0–25% inter-turn short circuit fault in the first branch of stator phase A winding is simulated.

The simulation results of air gap flux density before and after the fault are shown in Fig. 6.

It can be seen from Fig. 6 that after the fault, the air gap flux density of the generator affected by the short-circuit current is no longer symmetrical, and the air gap flux density of the area where the short-circuit winding is located has obvious distortion.

The air gap flux density of the generator before and after the fault is decomposed by FFT, and the result is shown in Fig. 7.

From the spectrum analysis results in Fig. 7, it can be seen that the air gap flux density only contains fundamental and odd harmonic components during normal operation of the generator. After the inter-turn short circuit fault, the air gap flux density of generator not only contains fundamental and odd harmonic components, but also even harmonic components.

5 Analysis of the Influence Factors of the Harmonic Component in the Air Gap Magnetic Field During the Inter-Turn Short Circuit of the Stator Winding

In order to study the influence factors of air gap flux density harmonic component after inter-turn short circuit fault of stator winding, In this section, the characteristics of air gap flux density change when the relative position of stator and rotor changes and the characteristics of air gap flux density change when the relative position of stator and rotor is constant are studied.

5.1 Influence of Relative Position Between Stator and Rotor on Air Gap Flux Density

In order to study the change characteristics of air gap magnetic density when the relative position of stator fault winding axis and magnetic pole axis changes with the same degree of inter-turn short circuit, The simulation of 0–25%inter-turn short circuit of the first branch winding of phase A is carried out. It is assumed that the relative position angle between the pole axis and the stator fault winding axis is α, Due to limited space, in this paper, the distribution of the magnetic field line of the generator is

Table 1 Main parameters of nuclear power half speed turbine generator

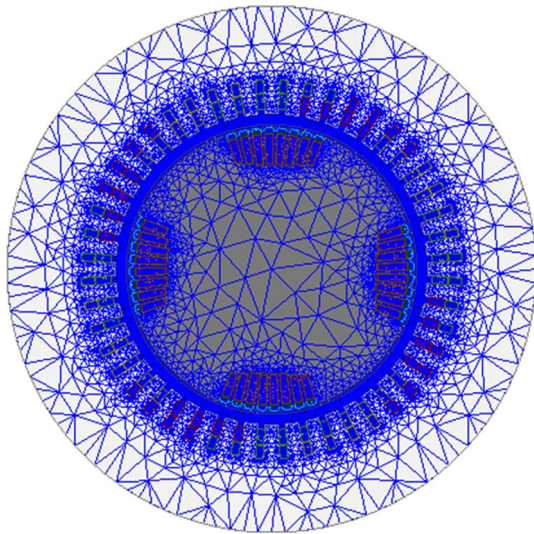| Parameter	Value	Parameter	Value
Rated capacity S_N/MVA	1407	Number of parallel branches of stator	2
Rated voltage U_N/kV	24	Synchronous reactance X_d/p.u	1.83
Power factor $cos\varphi$	0.9	Stator winding resistance R_s/Ω	0.000979
Number of pole-pairs p	2	Field winding resistance r_{fd}/Ω	0.0548

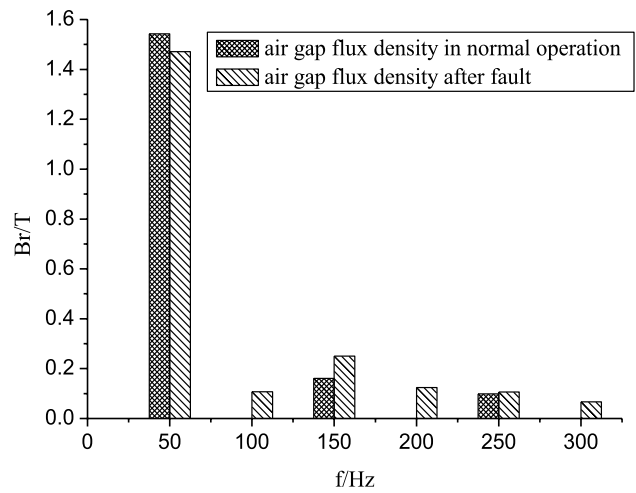**Fig. 5** Nuclear power generator finite element mesh cross-section figure

Fig. 7 Frequency spectrum of air gap flux density before and after stator winding inter-turn short circuit fault
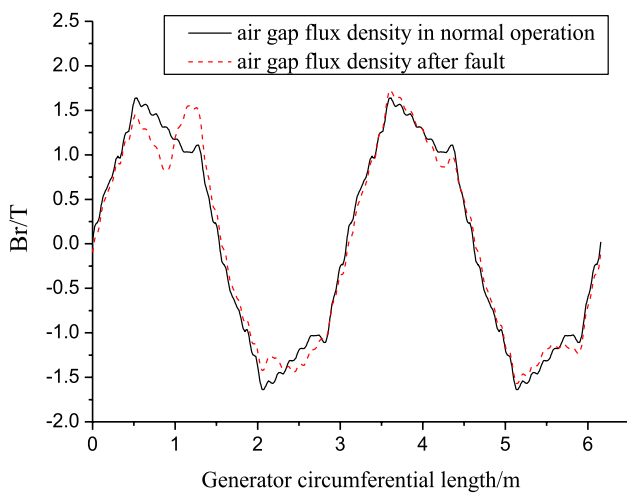

Fig. 6 Air gap flux density distribution before and after stator winding inter-turn short circuit fault
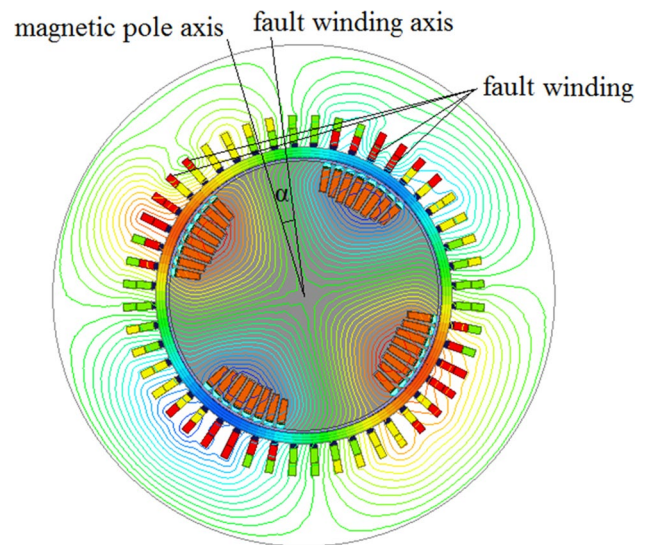

Fig. 8 Distribution of magnetic force line after stator winding inter-turn short circuit fault

given only when the magnetic pole axis is 9° ahead of the fault winding axis ($\alpha = 9°$). As it is shown in Fig. 8.

When the relative position of magnetic pole axis and fault winding axis changes under the stator winding inter-turn short circuit fault, the partial results of air gap magnetic density distribution are shown in Fig. 9.

As can be seen from Fig. 9, with the change of relative position angle α, the degree of air gap magnetic flux density distortion also changes.

The harmonic analysis of the air gap flux density at different α after the fault is carried out, and the results are shown in Fig. 10.

It can be seen from Fig. 10 that the distribution of the components of the air gap magnetic density has certain regularity with the change of α.

When the magnetic field in the area where the fault winding is located is the strongest, the fundamental component of air gap flux density is the smallest and the harmonic component is the largest.

5.2 Influence of Different Degree of Fault on Air Gap Flux Density

When the relative position between the axis of stator fault winding and the axis of magnetic pole is constant, the
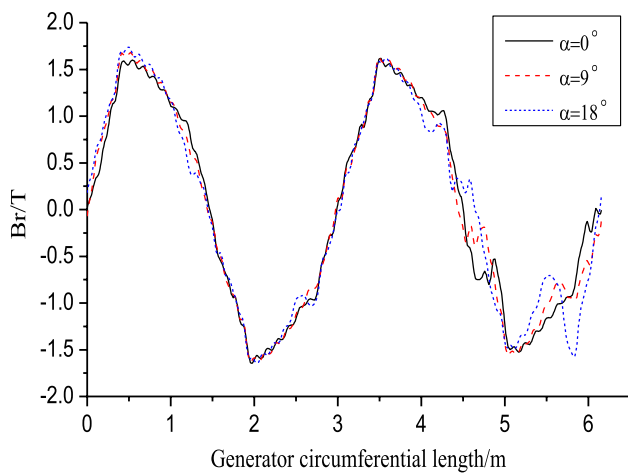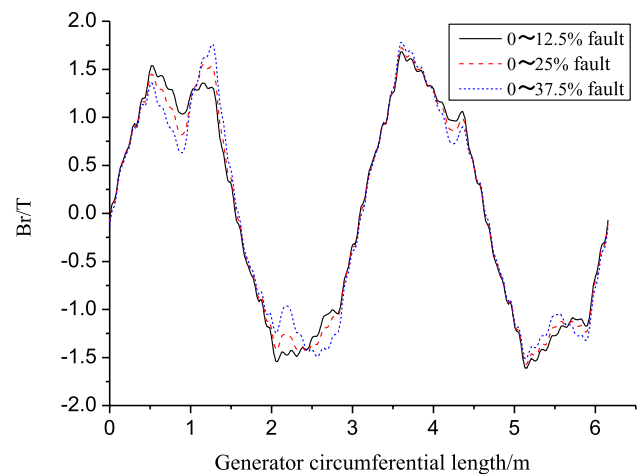
Fig. 9 Air gap magnetic density with change of α

Fig. 11 Air gap magnetic density distribution in different degree of fault

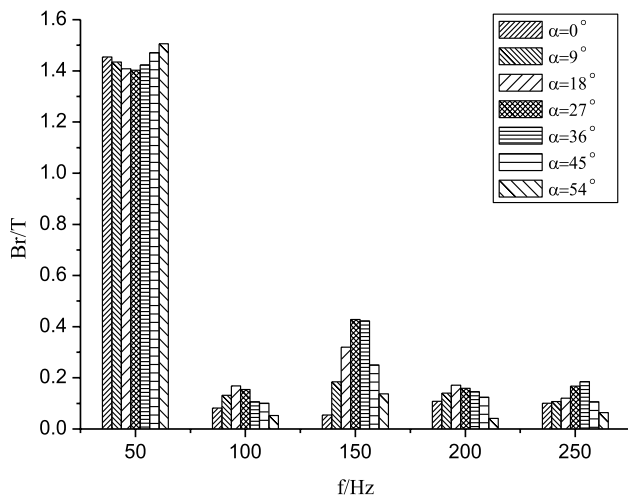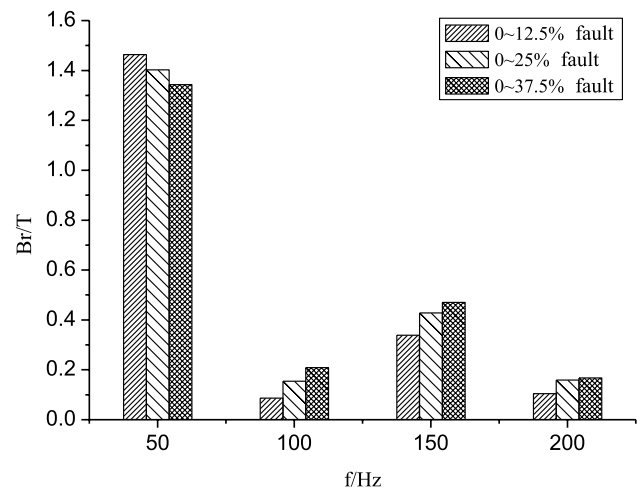**Fig. 10** Frequency spectrum of air gap flux density at different α

Fig. 12 Frequency spectrum of air gap flux density in different degree of fault

simulation of stator winding inter-turn short circuit fault in different degrees is carried out. The simulation results of air gap flux density in different degrees of fault are shown in Fig. 11.

The analysis results of air gap flux density spectrum under different degrees of fault are shown in Fig. 12. It can be seen from Fig. 12 that when the relative position between the axis of stator fault winding and the axis of magnetic pole is constant, The fundamental component of air gap flux density decreases with the increase of fault degree, while the harmonic component of air gap flux density increases with the increase of fault degree.

6 Analysis of Electromagnetic Torque in Stator Winding with Inter-turn Short Circuit

In order to study the harmonic components and influencing factors of the electromagnetic torque after the inter-turn short circuit fault in the stator winding of nuclear power generator, the analysis of the electromagnetic torque in the case of 0–37.5% inter-turn short circuit fault is carried out. The results of electromagnetic torque spectrum analysis are shown in Fig. 13.

From the spectrum analysis results in Fig. 13, it can be seen that the electromagnetic torque of nuclear power generator after stator winding inter-turn short circuit fault

contains not only the DC component in normal operation, but also the even harmonic component.

6.1 Influence of Different Degree of Fault on Electromagnetic Torque

The harmonic analysis of the electromagnetic torque under normal operation and different degrees of faults of the nuclear generator is shown in Fig. 14.

From the harmonic analysis results in Fig. 14, it can be seen that during fault operation, the electromagnetic torque generates even harmonic component in addition to DC component. In addition, with the increase of fault degree, the harmonic components of electromagnetic torque also increase. The DC component of the electromagnetic torque after the fault is obviously smaller than that of the normal operation, and the more serious the fault is, the smaller the DC component of the electromagnetic torque is.

6.2 Influence of Relative Position of Stator and Rotor on Electromagnetic Torque

An analysis is made of the electromagnetic torque when the relative position of the axis of the fault winding and the axis of the magnetic pole changes after the inter-turn short circuit fault of the stator winding. The results are shown in Fig. 15.

According to the simulation results in Fig. 15, when $\alpha = 27°$, the electromagnetic torque is the minimum. And this characteristic does not change with the degree of failure. It can be seen from Fig. 8 that the position of fault winding is exactly the maximum position of air gap Synthetic magnetic field. That is, the larger the air-gap synthetic magnetic field at the fault winding location, the smaller the electromagnetic
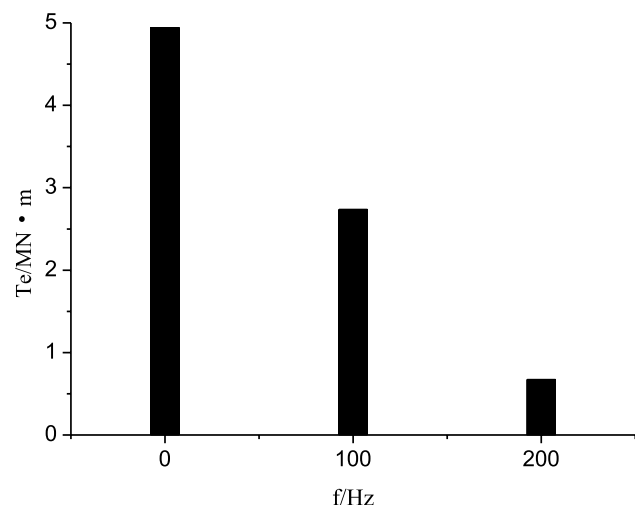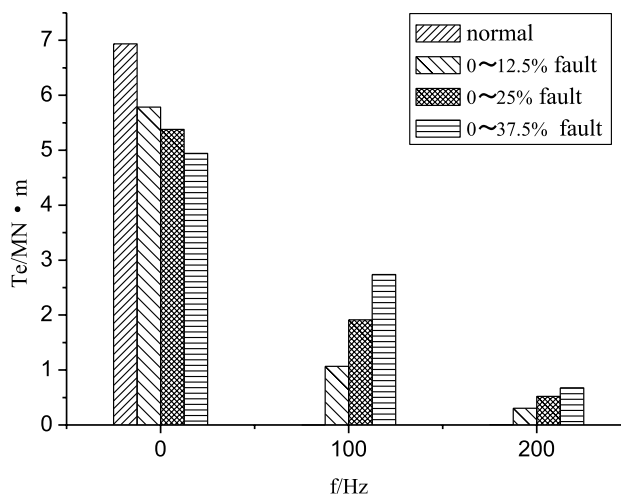

Fig. 14 Frequency spectrum of electromagnetic torque of generators before and after fault

torque. Therefore, this feature can be used to assist in determining the location of the faulty winding.

7 Conclusions

In this paper, the air gap magnetic field and electromagnetic torque of the generator in the case of an inter-turn short circuit in the stator windings of a nuclear power half-speed turbo-generator are studied. The main conclusions are as follows:

(1) When the inter-turn short circuit occurs in the stator winding of a nuclear power half speed turbo-generator, the air gap flux density does not only contain the odd
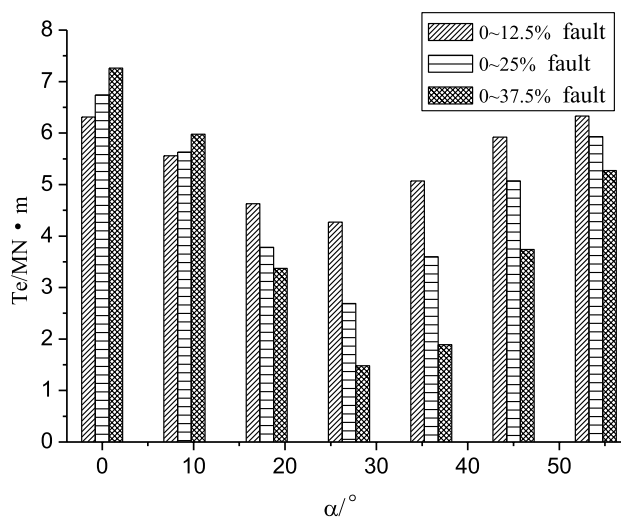

Fig. 13 Frequency spectrum of electromagnetic torque of generators after fault

Fig. 15 Electromagnetic torque of α change after fault

harmonic component in normal operation, but also the even harmonic component. At the same time, the change in air gap flux density is related to the relative position of the axis of the fault winding and the axis of the magnetic pole. The stronger the magnetic field in the area where the faulty winding is located, the smaller the fundamental component of the air-gap flux density and the larger the harmonic component. When the relative position of the fault winding axis and the magnetic pole axis is constant, the more serious the fault is, the more serious the magnetic field distortion, the smaller the fundamental component of the air-gap flux density, and the larger the harmonic component.

(2) When the inter-turn short circuit fault of stator winding occurs, in addition to the DC component, the electromagnetic torque also generates an even harmonic component. And the DC component decreases with the increase of fault degree, while the harmonic component increases with the increase of fault degree. The larger the air gap synthetic magnetic field at the location of the fault winding, the smaller the electromagnetic torque. And this characteristic does not change with the fault degree.

Based on the existing research results, this paper further analyzes the change characteristics and influencing factors of the air gap magnetic field and electromagnetic torque after the inter-turn short circuit of the stator windings of a nuclear power generator. It is of certain significance to realize the fault diagnosis and location using the electromagnetic torque after the fault.

References

1. Meng L, Luo YL, Liu XF, Yang JF, Chi YB (2005) A case study of electromagnetic force distribution on rotor core surface of turbo-generator. Proc CSEE 25:81–86
2. He YL, Wang FL, Tang GJ, Jiang HC, Yuan XH (2017) Effect of stator inter-turn short circuit position on electromagnetic torque of generator with consideration of air-gap eccentricity. Trans China Electrotech Soc 32:11–19
3. Sarikhani A, Mohammed OA (2013) Inter-turn fault detection in PM synchronous machines by physics-based back electromotive force estimation. IEEE Trans Industr Electron 60:3472–3484
4. Wan ST, Wu WJ, He YL, Li H (2009) Analysis on vibration characteristic when eccentric vibration under stator winding inter-turn short circuit fault. J North China Electric Power Univ 36:86–93
5. He YL, Wang FL, Tang GJ, Jiang HC, Yuan XH (2017) Effect of stator inter-turn short circuit position on stator vibration of generator. J Vib Eng 30:679–687
6. Xie Y, Liu HD, Li F, Liu HS (2017) Effect of rotor eccentricity and stator short circuit faults on magnetic field and electromagnetic vibration characteristics of synchronous generator. J Cent South Univ (Sci Technol) 48:2034–2043
7. Wan ST, Li HM, Xu ZF, Li YG (2004) Analysis of generator vibration characteristic on stator winding inter-turn short circuit fault. Proc CSEE 24:157–161
8. Sun YG, Yu XW, Wei K, Huang ZG, Wang XH (2014) A new type of search coil for detecting inter-turn faults in synchronous machines. Proc CSEE 34:917–924
9. Zhao HS, Ge BJ, Tao DJ, Yang K, Xing G (2018) Investigation on stator winding inter-turns short circuit fault diagnosis. J Harbin Univ Sci Technol 23:99–104
10. Xiao SY, Ge BJ, Tao DJ, Liu ZH (2018) Calculation of rotor dynamic electromagnetic force of synchronous generator under the stator winding interturn short circuit fault. Trans China Electrotech Soc 33:2956–2962
11. Ye ZJ, You BQ, Rosendahl J, Kuling ST (2013) Fault characteristic study based on FLUX 2D for large synchronous generators with stator winding inter-turn short circuits under rated operating conditions. Proc CSEE 33:125–132
12. Fang HW, Xia CL, Xiu J (2007) Analysis of generator eletromagnetic torque on armature winding inter-turn short circuit fault. Proc CSEE 27:83–87
13. Fang HW, Xia CL, Li GP (2009) Analysis of synchronous generator electro-magnetic torque and vibration with armature winding fault. J Tianjin Univ 42:322–326
14. Zhao HS, Ge BJ, Tao DJ, Han JC, Wang LK (2018) Influence of stator internal short-circuit fault on rotor eddy current losses in nuclear power turbo-generator. Electric Machines and Control 22:17–25
15. Hu MQ, Huang XL (2003) Numerical calculation method of motor performance and its application. Southeast University Press, Nanjing, pp 173–179
16. Hu J, Luo YL, Liu XF et al (2009) Influence of calculation parameters of time-stepping finite element method on simulation results in turbo-generators large disturbance process. Proc CSEE 29:59–66

Publisher's Note Springer Nature remains neutral with regard to jurisdictional claims in published maps and institutional affiliations.

Peng Xin received the Ph.D. degree from Harbin University of Science and Technology in 2018, and now he works at Jilin Institute of chemical technology. He is mainly engaged in the research of generator fault diagnosis and dynamic transition process.

Baojun Ge is the professor of Harbin University of Science and Technology . His research interest is the basic theory and operation research of large electromechanical energy conversion device.

Dajun Tao received the Ph.D. degree from Harbin University of Science and Technology in 2013. He is mainly engaged in the research of dynamic transient process and stability of large generator.

Pin Lv received the Ph.D. degree from Harbin University of Science and Technology in 2017, and now she works at Heilongjiang University of Science and Technology. Her research interest is asymmetric operation of generator.